第三型应变时效的提出与研究进展*

王建军[1]，袁康博[2]，张晓琼[1]，王瑞丰[2]，高　猛[2]，郭伟国[2]

（1. 太原理工大学机械与运载工程学院，山西 太原 030024；

2. 西北工业大学航空学院，陕西 西安 710072）

摘要： 第三型应变时效现象的发现使得传统的对于金属塑性流动行为的认识、位错的热激活理论以及常见的金属热粘塑性本构模型均需要进一步完善。为了系统地认识第三型应变时效，首先介绍了第三型应变时效现象区别于静态应变时效和 Portevin-Le Chatelie 动态应变时效的宏观特征，其次，对第三型应变时效的微观机理以及第三型应变时效与 Portevin-Le Chatelier 动态应变时效、蓝脆现象以及机械波谱的关联性进行了系统总结。最后，介绍了包含第三型应变时效的金属热黏塑性本构模型的发展。

关键词： 应变时效；温度；应变率；微观机理；本构模型

中图分类号： O347.3　　　**国标学科代码：** 13015　　　**文献标志码：** A

Proposition and research progress of the third-type strain aging

WANG Jianjun[1], YUAN Kangbo[2], ZHANG Xiaoqiong[1], WANG Ruifeng[2], GAO Meng[2], GUO Weiguo[2]

（1. *College of Mechanical and Vehicle Engineering, Taiyuan Universtiy of Technology,*

Taiyuan 030024, *Shanxi, China;*

2. *School of Aeronautics, Northwestern Polytechnical University, Xi'an* 710072, *Shaanxi, China*）

Abstract: The traditional knowledge of plastic flow behavior of metal, dislocation activation theory, and thermoviscoplastic constitutive model of metal needs a further perfection due to the occurrence of third-type strain aging. Third-type strain aging leads to a bell-shaped flow stress-temperature curve, that is, the flow stress first increases as temperature increases, and after a peak value is reached, it decreases with further increase of temperature. Third-type strain aging occurs at both low and high strain rates. The bell-shaped segment induced by third-type strain aging on the flow stress-temperature curve shifts to higher temperature region as strain rate increases. In order to develop a systematic understanding of the third-type strain aging, firstly, macro characteristics of third-type stain aging effect that was distinguished from static strain aging effect and Portevin-Le Chatelier dynamic strain aging effect were introduced. Then, the micro mechanism of third-type strain aging and correlation of third-type strain aging, Portevin-Le Chatelier dynamic strain aging, blue brittleness phenomenon, and internal friction were systematically concluded. Third-type strain aging, Portevin-Le Chatelier dynamic strain aging, blue brittleness phenomenon, and mechanical spectroscopy are all resulted from the interaction of mobile dislocations with diffusion atoms. Third-type strain aging, Portevin-Le Chatelier dynamic strain aging, and blue brittleness phenomenon are different manifestations of dynamic strain aging. Third-type strain aging can be considered as another mode of mechanical spectroscopy. The common constitutive models are able to capture the plastic behavior of many metals under the coupling influence of strain rate and temperature in some cases. However, these thermoviscoplastic constitutive models do not take the effect of third-type strain aging into consideration, and they cannot describe the thermoviscoplastic behavior including the third-type strain aging effect. To accurately describe the plastic behavior of metals, some constitutive models including the effect of third type strain aging were

---

proposed. The development of the thermoviscoplastic constitutive model of metal considering the effect of third type strain aging was finally introduced.

Keywords: strain aging; temperature; strain rate; microscopic mechanism; constitutive model

在对金属材料在很宽温度、很宽应变率范围内的塑性流动行为进行测试时, 会发现: 在相同的应变率下, 随着温度的升高, 流动应力应变曲线不会出现我们通常认为的下降, 而是会整体曲线或较大部分反而上升, 如图 1(a)所示, 图中 T_1、T_2 和 T_3 分别为三条应力应变曲线的试验温度, 表现在对应的流动应力-温度曲线上为出现一反常应力峰[1-6]。这种金属材料随温度升高出现的强化现象与塑性变形中的 Portevin-Le Chatelier(PLC)动态应变时效类似, 即应变和时效同时发生, 都属于动态应变时效现象, 但是二者的宏观表现完全不同, PLC 动态应变时效表现为应力-应变曲线上的锯齿流动现象[7], 如图 1(b)所示。动态应变时效现象的发现最早可以追溯到 Le Chatelier 在 1909 年在低碳钢的高温变形中首次发现了锯齿流动现象, 之后 Portevin 和 Le Chatelier 在 "硬铝" 的常温变形中发现了相似现象, 这种锯齿流动现象从此被命名为 PLC 效应[7]。鉴于这种流动应力随温度变化在曲线上出现的反常应力峰现象在形式上有别于静态应变时效[8-9](见图 1(c))和 PLC 动态应变时效, Wang 等[6] 在 2015 年首次将这一现象命名为 "第三型应变时效"(third-type strain aging, 简称 3rd SA)。学者们在研究多种金属材料的塑性流动行为中均发现了类似的反常应力峰现象, 并沿用了第三型应变时效这一命名[10-15]。第三型应变时效现象的出现具有普遍性, 不仅在 BCC、FCC 和 HCP 多晶金属中发现了这一现象[16-20], 而且在单晶金属中也出现了这一现象[21-23]。

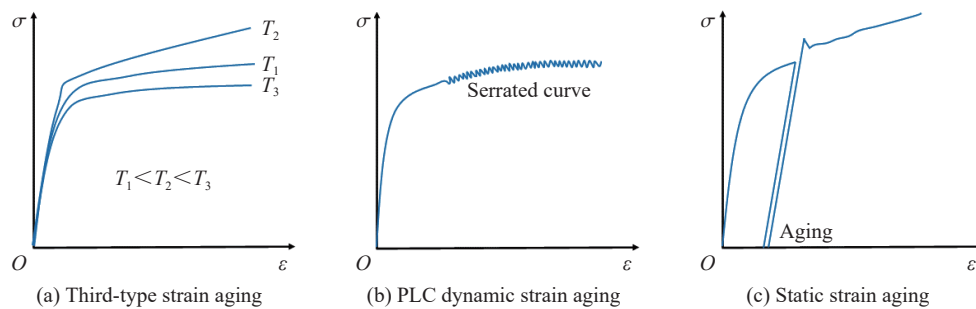图 1　三种应变时效的表现形式

(a) Third-type strain aging　　(b) PLC dynamic strain aging　　(c) Static strain aging

Fig. 1　Manifestation of the three kinds of strain aging

第三型应变时效现象的发现, 使得传统的金属材料力学性能随温度升高出现热软化及其相关位错的热激活理论不能准确解释金属材料力学行为随温度的变化规律。常见的经验型本构关系和基于位错热激活理论的物理概念本构关系都不能很好地描述金属的塑性流动行为。为此, 本文中从第三型应变时效现象的宏观特征、微观机理以及考虑第三型应变时效的本构关系三个方面来系统介绍第三型应变时效。

1　第三型应变时效现象的宏观特征

为了直观地分析第三型应变时效现象, 将不同温度下的应力应变曲线转换为流动应力随温度变化的曲线, 可以发现: 在同一应变率下, 随着温度的升高, 流动应力先减小, 当温度达到某一值时, 流动应力随着温度的升高出现了反常的增长, 直至达到一峰值应力, 随着温度的继续升高, 流动应力随温度的升高而下降。在某一温度区域内, 流动应力随温度变化的曲线上出现了有第三型应变时效引起的反常应力峰, 如图 2[1, 24] 所示。对于奥氏体和铁素体不锈钢, 在准静态下应力峰出现的温度范围约为 0.3～0.5 倍的熔点温度[25], 对于双相不锈钢, 应力峰出现的温度为 0.35 倍的熔点温度[26]。从图 2 中可以看出, 应力峰出现的温度随应变率的增大而移向更高温度。对于 Q235B 钢, 在 0.001 s⁻¹ 应变率下, 应力峰出现的温

度为 0.31 倍的熔点温度; 在 800 s^{-1} 应变率下, 应力峰出现的温度为 0.52 倍的熔点温度; 当应变率为 7 000 s^{-1} 时, 应力峰出现的温度为 0.56 倍的熔点温度[6]。为了定量描述应力峰随应变率的变化规律, Guo 等[3]、Wang 等[6]、孟卫华等[27-28] 建立了相关的物理模型。
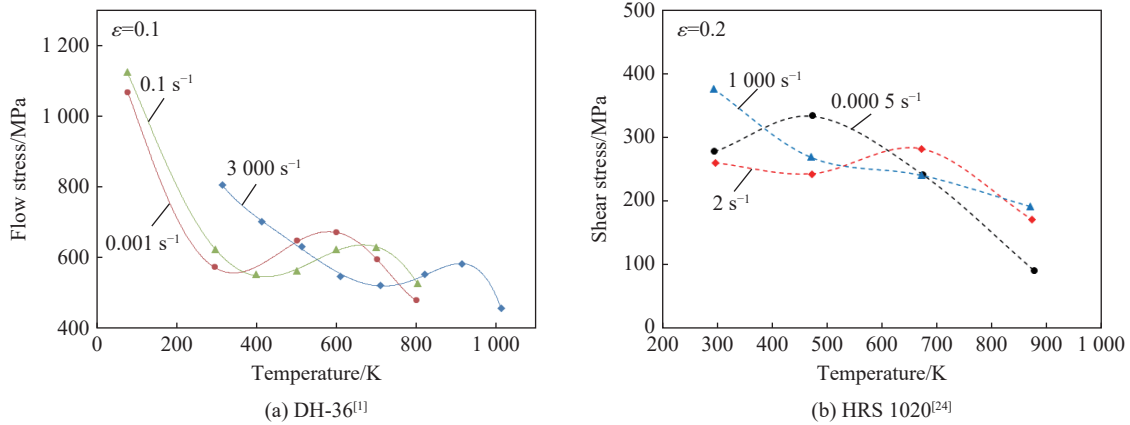

图 2　不同应变率下流动应力随温度变化曲线

Fig. 2　Variation of flow stress with temperature at different strain rates

　　第三型应变时效的出现往往伴随着 PLC 动态应变时效现象, 并且 PLC 动态应变时效通常出现在应力峰上升部分对应的温度区域内[6, 29-31]。根据 PLC 动态应变时效引起的锯齿形状特征, 通常把锯齿形状分为 A、B、C 三种类型[32-34]。PLC 动态应变时效同时会引起试样表面出现局部的变形带 (Luders 带), 随着应力增大, 变形带会沿着试样移动[34-35]。A 型锯齿波一般在较小的应变和较低的温度时出现, A 型锯齿波的一个重要特点是: Luders 带在逐渐升高的外力作用下向前移动; B 型锯齿波一般出现在较高的温度或较低的应变率下, 并且 Luders 带生成后并不扩展; C 型锯齿波的形状介于 A 型与 B 型之间, Luders 带生成后并不扩展, 并且不断有新的 Luders 带生成[34]。Sakthivel 等[36] 通过对高温合金 Hastelloy X 在宽温域、不同应变率下的锯齿流动行为进行测试, 分析了温度和应变率对高温合金 Hastelloy X 锯齿流动行为的影响。Roy 等[37] 对奥氏体高温合金 C-276 在宽温域、不同应变率下的锯齿流动行为进行了测试和分析, 并通过透射电镜观察发现: 锯齿流动出现时位错密度增大。Karabulut 等[38] 通过改变中碳钢中钒的含量来研究钒含量对第三型应变时效的影响。Gündüz 等[39] 研究了不同的热处理对第三型应变时效引起的反常应力峰的影响。Ganesan 等[5] 研究了 316LN 奥氏体不锈钢中氮含量对动态应变时效行为(包括锯齿流动出现的温度和锯齿流动出现的临界应变)的影响, 并认为氮溶质原子是引起 316LN 奥氏体不锈钢中出现动态应变时效的原因。Xiao 等[40] 通过热处理来改变 DH-36 钢中自由碳原子的含量, 进而分析其对第三型应变时效引起的反常应力峰宏观特征的影响。Yuan 等[41] 通过测试三种不同热处理状态下的激光金属沉积 Inconel 718 合金在宽温度和应变率范围内的塑性流动行为, 发现时效处理后沉淀强化合金材料的第三型应变时效引起的反常应力峰明显降低[41], 沉积态合金的反常应力峰也随着应变率的升高而降低[42]。

2　第三型应变时效的微观机理

　　在金属的塑性变形过程中, 位错的运动并不是连续的, 它们在运动时将被暂时阻挡在短程障碍物 (如溶质原子) 之前, 等待热激活以克服障碍物, 再前进到下一个障碍物[43]。在位错在障碍前的等待期间, 溶质原子向位错扩散, 在位错周围形成溶质原子气团, 对运动位错"钉扎", 阻碍了位错的运动(见图 3), 在宏观上表现为金属流动应力增大[44]。目前, 对溶质原子扩散至运动位错周围的方式还存在争议。Cottrell 等[45] 认为变形诱导的空位可以帮助溶质原子的扩散; Cuddy 等[46]、Schwarz 等[47] 认为溶质原子借助林位错管道扩散至运动位错周围, 形成溶质原子气团, 对运动位错"钉扎", 而不需要借助于空

穴, 也就是说管道扩散是引起动态应变时效的主要机制。Picu 等[48] 研究发现, 如果不借助于空位, 管道扩散的速度会太慢。对于钢, 如果不含有足够的合金元素, 如 Al、V、Nb、Ti, 则碳原子和氮原子不能全部形成碳化物和氮化物, 因此, 由于自由碳原子和氮原子与位错的相互作用, 合金钢的塑性流动行为中会出现应变时效[6]。通过计算 18-8 奥氏体不锈钢动态应变时效过程的激活能, Peng 等[49] 发现: 在低温下, 动态应变时效是由 C、Ni 溶质原子气团和位错的相互作用引起的, 而在高温下, 动态应变时效则是由 C、Cr 溶质原子气团和位错的相互作用引起的。Cuddy 等[46] 发现: 对于铁基合金, 置换溶质原子(O、Si、Mn、Ni、Ru、Rh、Re、Ir 和 Pt)与位错的相互作用是引起动态应变时效的主要原因。对于镁合金 AZ91, Al 原子被认为是引起动态应变时效的主要溶质原子, 而 Zn 原子被作为 Al 原子扩散的催化剂[50]。
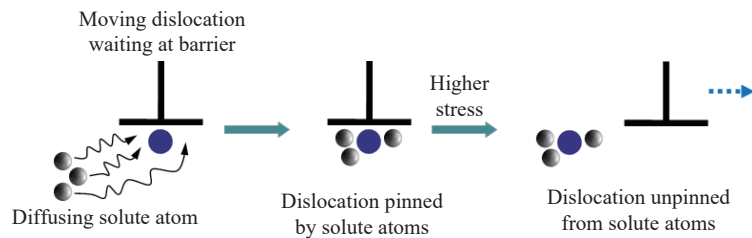

图 3　扩散的溶质原子对运动位错的钉扎引起的第三型应变时效的示意图

Fig. 3　Schematic of third-type strain aging caused by dislocation pinning by diffused solute atom

由于热量可以为点缺陷的运动提供能量, 因此, 温度可以影响溶质原子和空位的运动, 而应变率可以影响位错的数量和运动[51]。当温度和应变率达到某种关系时, 在位错周围会形成溶质原子气团, "钉扎"位错, 阻碍其运动[43, 52]。在低温高应变率下, 溶质原子的扩散速度低于对应的位错运动速度, 第三型应变时效不会发生。在高温低应变率下, 溶质原子气团随着位错运动, 溶质原子的扩散速度高于对应的位错的运动速度, 溶质原子气团不会对位错"钉扎", 第三型应变时效同样不会发生[45, 53]。

早在 19 世纪, 人们就发现, 在机械加工过程中, 当低碳钢被加热到表面变蓝时会变得很脆, 这一现象被称为"蓝脆", 原因在于, 材料在塑性变形过程中, 扩散的溶质原子对位错的钉扎, 造成了材料变形阻力的增加。随着变形阻力的增加, 材料内的应力水平也会更高, 引起微裂纹的形成和增殖, 最终导致材料韧性降低[25, 54-55]。伴随着第三型应变时效引起的反常应力峰, 材料的韧性也通常随温度升高而降低, 即出现蓝脆现象, 在该温度区域内, 韧性随温度变化呈现一低谷[17, 31, 56]。对于 BCC 铁, 在出现蓝脆温度区域内, 动态应变时效是由运动位错和碳或氮溶质原子的相互作用引起的[57]。Koyama 等[58] 研究了不同碳含量对 Fe-Mn-C 奥氏体不锈钢力学行为中表现出来的动态应变时效引起的蓝脆现象的影响规律。与应变率对第三型应变时效现象的影响相似, 随着应变率的增大, 蓝脆现象出现的温度区域移向更高的温度区域[31]。PLC 效应、第三型应变时效和蓝脆现象都是由运动位错与扩散的溶质原子的相互作用引起的, 被认为是动态应变时效的三种表现形式[6]。

在动态应变时效的温度区域内, 多种金属材料的内耗随温度变化曲线出现了 Snoek 内耗峰[59]。Schwink 等[60] 认为金属内耗峰产生的机理可用来解释 PLC 效应。并且已有的研究结果表明, 对于铁碳合金, 当振动频率为 1 Hz 时, 内耗峰出现在 470~590 K 的温度范围内[61-64], 该温度范围与准静态下动态应变时效出现的温度范围接近。随着频率增大, 内耗峰会移向更高的温度[63, 65-66]。Wang 等[6] 和郭伟国等[67] 通过研究发现, 内耗峰出现的温度随频率的变化规律与第三型应变时效出现的温度随应变率的变化规律相同。内耗峰和金属塑性变形中出现的第三型应变时效都是由相同的微观机理引起的, 并且二者有着相似的宏观特征。因此, 第三型应变时效被认为是机械波谱的另一种表现形式。彭开萍等[68] 对 3004 铝合金在"反常"锯齿屈服的温度区域进行了内耗试验, 并结合激活能的计算、内耗研究、微观组织观察和能谱分析, 探讨"反常"锯齿屈服的机理与物理本质。Lee 等[69] 通过内耗试验分析了孪晶诱导塑性钢(Fe-18%Mn-0.6% C 和 Fe-18% Mn-1.5% Al-0.6% C)在常温下出现 PLC 锯齿流动的原因。Karlsen 等[70] 通过对 AISI 316 NG 奥氏体不锈钢进行不同温度下预应变后的内耗试验发现: 在动态应变

时效温度区域内预应变后的 Snoek 内耗峰的高度显著增大。Ivanchenko 等[71]对退火后的镍基高温合金 Inconel 600 进行了内耗试验,在 620～670 K 温度范围内出现了碳原子引起的 Snoek 内耗峰,而当对镍基高温合金 Inconel 600 在动态应变时效出现的温度(423 K)下首先进行预拉伸,而后进行内耗试验时,发现其内耗峰明显增大。

综上所述,第三型应变时效、PLC 效应和蓝脆现象都是由运动位错与扩散的溶质原子的相互作用引起的,被认为是动态应变时效的三种表现形式。

3　包含第三型应变时效的金属热黏塑性本构模型

常见的描述金属塑性流动行为的热黏塑性本构模型可分为经验型/唯象本构模型和物理概念本构模型。经验型本构模型最常见的有 Johnson-Cook 本构模型(J-C 模型)[72-74],J-C 模型是一种纯经验型或者半经验型本构模型,由于其形式简单而被广泛应用于工程实践中,并被嵌入到 ANSYS、ABAQUS 等有限元软件中。物理概念本构模型主要包括 Zerilli-Armstrong 模型(Z-A 模型)[75]、力阈值应力本构模型(MTS 模型)[76]、Bonder-Partom 模型(B-P 模型)[77]、Nemat-Nasser 物理概念本构模型[1-2, 78-79]以及其他具有物理意义的本构模型[73, 80],这些本构模型都已被认可和广泛应用。Z-A 模型是基于位错动力学的概念提出的、分别针对 FCC 和 BCC 金属的塑性流动本构模型,模型中考虑晶粒尺寸的影响。MTS 模型是基于位错的热激活运动理论建立的,它将流动应力和力阈值应力作为内状态变量与应变和应变率相关联。B-P 模型是基于连续介质力学和唯象学的基本概念建立起来的。Nemat-Nasser 物理概念本构模型是基于位错的动力学基本理论建立起来的,其将塑性流动应力分为热激活部分和非热部分。近几年,Gao 等[81]研究了 FCC 金属在高应变率下运动位错密度的演化,并建立了相关的本构模型。Khan 等[82]建立了可以描述 2024-T351 铝合金的依赖于温度和应变率的唯象本构模型。

研究表明,以上金属热黏塑性本构模型可以很好地描述金属材料在不同温度、不同应变率下的塑性流动行为,并且这些本构模型在工程中均得到了广泛的应用。但是,这些模型都没有考虑金属塑性流动行为中出现的第三型应变时效现象,也就是说,金属塑性流动行为出现的第三型应变时效现象使得现有金属热黏塑性本构模型均不再适用。为了能描述金属塑性流动行为中普遍存在的第三型应变时效现象,学者们基于运动位错与溶质原子的相互作用建立了可以描述该行为的物理概念本构模型[24, 83],但是由于第三型应变时效过程较为复杂,使得建立的这类模型极为复杂。通常,这类模型会包含大量的参数,使得拟合过程也极为困难。为了能描述第三型应变时效对金属材料塑性流动行为的影响,唯象第三型应变时效模型被广泛采用[3, 6, 27-28, 84-87]。Lee 等[86]建立了半经验型的第三型应变时效模型,但该模型并未考虑应变率对第三型应变时效的影响。Lee 等[85]和 Guo 等[3]、孟卫华等[27-28]、Su 等[87]在 Nemat-Nasser 物理概念本构模型的基础上,考虑了第三型应变时效的影响以及第三型应变时效随应变率的变化规律,建立了可以描述金属塑性流动行为中出现的反常应力峰现象的塑性流动本构模型,初步完善了金属热黏塑性本构模型。Shen 等[88]利用唯象第三型应变时效模型建立了可以描述金属各向异性、热软化和第三型应变时效现象的金属热黏塑性本构模型,如图 4 所示。Wang 等[6]结合第三型应变时效发生的机理(即运动位错与溶质原子的相互作用)及其宏观特征,建立了包含第三型应变时效现象的金属塑性流动本构模型。图 5 所示为本构模型预测得到的 Q235B 钢的流动应力随温度和应变率变化的情况,从图中可以看出,第三型应变时效引起的应力峰如同"山脊"出现在时效温度区域内,并且随着应变率增大,应力峰高度降低,其出现的温度区域移向了更高的温度区域。郭扬波等[89]考虑位错与位错芯内的溶质原子 (位错芯气团) 的相互作用,在 Z-A 热黏塑性本构模型的基础上,加入位错和位错芯气团的相互作用的影响,建立了一种可定量描述第三型应变时效现象的本构模型。Song 等[10]利用 Wang 等[6]建立的第三型应变时效模型建立了包含第三型应变时效的金属热黏塑性本构模型。Song 等[11]、Voyiadjis 等[90-91]基于修正的 Voyiadjis-Abed 模型建立了包含第三型应变时效的热黏塑性本构模型。Li 等[18]通过机器学

习的方法确定了修正的 J-C 本构模型, 模型可以描述 DP800 钢在不同温度和应变率下的塑性流动行为, 但是文中所研究的温度范围为 20～300 ℃, DP800 钢塑性流动行为并没有表现出完整的第三型应变时效, 如图 6 所示。Yuan 等[41] 针对三种不同热处理状态下激光沉积 Inconel 718 合金, 将 Wang 等[6] 建立的第三型应变时效模型引入考虑热处理引起的微观结构演化的物理本构模型。拟合出流动应力的动态应变时效分量的本构参数, 结合微观组织分析认为, 沉淀强化金属材料中不同尺寸的沉淀相对第三型应变时效具有不同的影响机制。当运动位错切过尺寸较小的强化相时, 强化相与钉扎原子的共同作用使第三型应变时效现象更为明显; 而当运动位错绕过尺寸交大的强化相时, 部分钉扎原子被保留在围绕强化相的位错环内, 导致运动位错上钉扎原子浓度降低, 从而减弱了第三型应变时效现象。
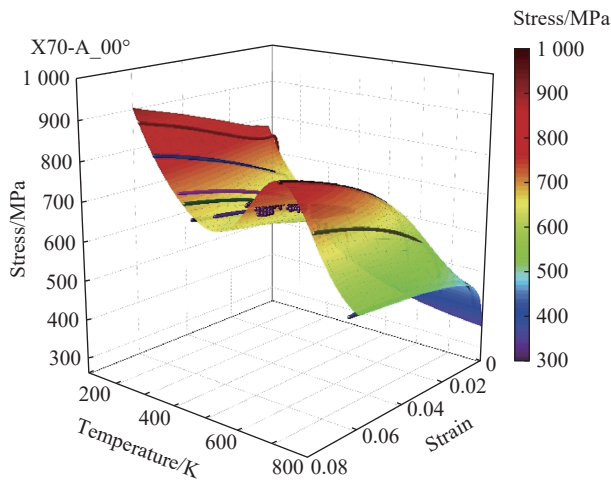
图 4　API X70 管线钢塑性流动行为中出现的第三型应变时效现象及本构模型预测结果[88]

Fig. 4　Third type strain aging phenomenon in the plastic flow behavior of API X70 pipeline steel and prediction results of constitutive model[88]

图 5　本构模型预测得到的 Q235B 钢在应变为 0.1 下的流动应力随温度和应变率变化的情况[6]

Fig. 5　Constitutive model predicted variation of flow stress at the strain of 0.1 with temperature and strain rate for Q235B steel[6]

(a) $\dot{\varepsilon}$=0.001 s^{-1}

(b) $\dot{\varepsilon}$=1 000 s^{-1}

图 6　通过机器学习得到的 DP800 钢的流动应力随温度和等效应变率变化的情况[18]

Fig. 6　Variation of flow stress with temperature and strain rate obtained with machine learning for DP 800 steel[18]

4　结　论

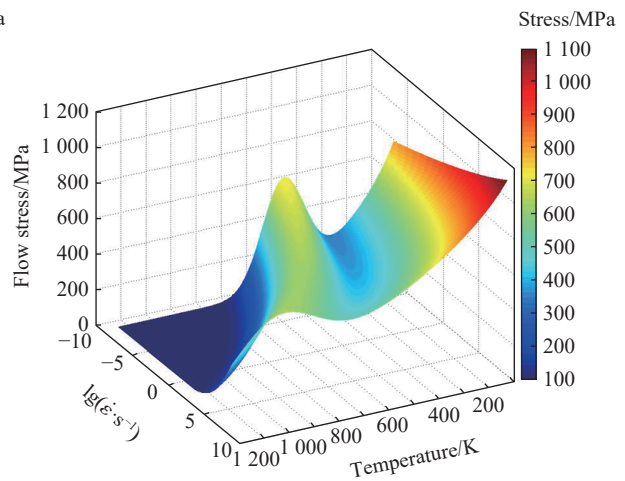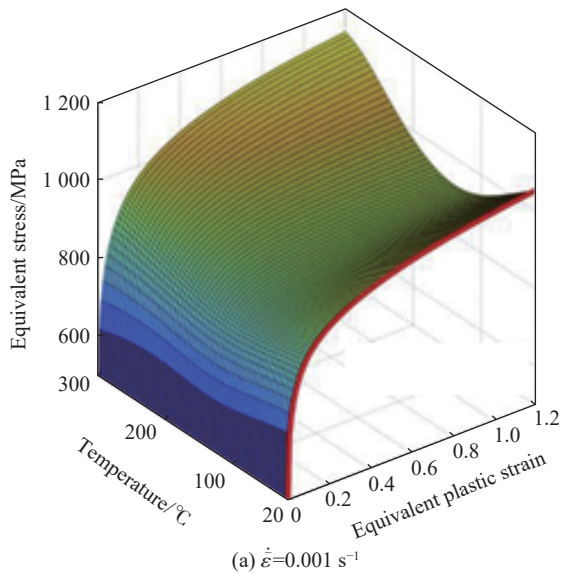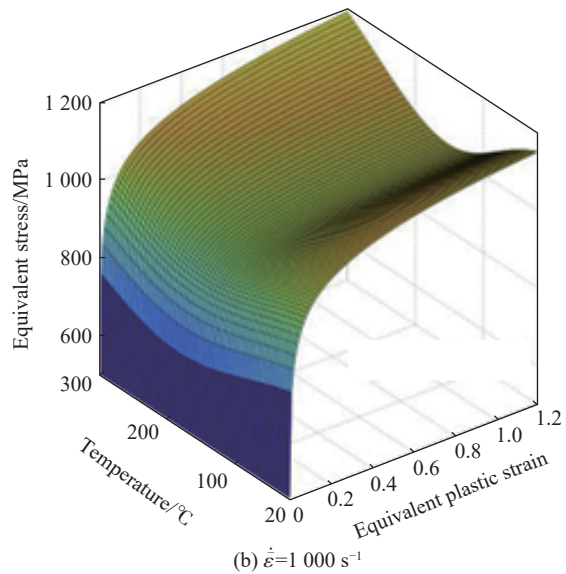随着金属材料的发展以及对晶体位错理论的不断认识, 传统的金属材料力学性能随温度升高出现的热软化及其相关的位错的热激活理论并不能完全反映金属材料力学行为随温度的变化规律。通常认为金属材料的流动应力随着温度的升高而降低, 但在金属材料的实际应用中或对金属材料力学行为进行试验测试时会发现, 在某一温度范围内, 其流动应力随温度变化的曲线上会出现一反常应力峰, 即第三型应变时效现象。第三型应变时效被认为是由运动位错与扩散溶质原子的相互作用引起的, 而溶质原子的扩散需要借助于空位或/和林位错管道。第三型应变时效、PLC 动态应变时效和蓝脆现象都是由运动位错与扩散的溶质原子的相互作用引起的, 是动态应变时效的三种表现形式, 并且第三型应变时效被认为是机械波谱的另一种表现形式。第三型应变时效现象的出现使得常见的本构模型不能描述金属的塑性流动行为, 具有物理概念的包含第三型应变时效的本构模型由于形式过于复杂而并未得到广泛应用, 而近几年基于第三型应变时效的机理和宏观特征建立的半经验型的包含第三型应变时效的本构模型受到了广泛重视。

参考文献:

[1]　NEMAT-NASSER S, GUO W G. Thermomechanical response of DH-36 structural steel over a wide range of strain rates and temperatures [J]. Mechanics of Materials, 2003, 35(11): 1023–1047. DOI: 10.1016/S0167-6636(02)00323-X.

[2]　NEMAT-NASSER S, GUO W G. Thermomechanical response of HSLA-65 steel plates: experiments and modeling [J]. Mechanics of Materials, 2005, 37(2): 379–405. DOI: 10.1016/j.mechmat.2003.08.017.

[3]　GUO W G, GAO X S. On the constitutive modeling of a structural steel over a range of strain rates and temperatures [J]. Materials Science and Engineering: A, 2013, 561: 468–476. DOI: 10.1016/j.msea.2012.10.065.

[4]　CORNET C, WACKERMANN K, STÖCKER C, et al. Effects of temperature and hold time on dynamic strain aging in a nickel based superalloy [J]. Materials at High Temperatures, 2014, 31(3): 226–232. DOI: 10.1179/1878641314Y.0000000018.

[5]　GANESAN V, LAHA K, NANDAGOPAL M, et al. Effect of nitrogen content on dynamic strain ageing behaviour of type 316LN austenitic stainless steel during tensile deformation [J]. Materials at High Temperatures, 2014, 31(2): 162–170. DOI: 10.1179/1878641314Y.0000000009.

[6]　WANG J J, GUO W G, GAO X S, et al. The third-type of strain aging and the constitutive modeling of a Q235B steel over a wide range of temperatures and strain rates [J]. International Journal of Plasticity, 2015, 65: 85–107. DOI: 10.1016/j.ijplas.2014.08.017.

[7]　PORTEVIN A, LE-CHATELIER H. Heat treatment of aluminium-copper alloys [J]. Transaction of the American Society of Steel Treating, 1924, 5: 457–478.

[8]　MOTT N F, NABARRO F R N. Report of a conference on the strength of solids [M]. London: Physical Society, 1948.

[9]　COTTRELL A H, BILBY B A. Dislocation theory of yielding and strain ageing of iron [J]. Proceedings of the Physical Society: Section A, 1949, 62(1): 49–62. DOI: 10.1088/0370-1298/62/1/308.

[10]　SONG Y, GARCIA-GONZALEZ D, RUSINEK A. Constitutive models for dynamic strain aging in metals: strain rate and temperature dependences on the flow stress [J]. Materials, 2020, 13(7): 1794. DOI: 10.3390/ma13071794.

[11]　SONG Y, VOYIADJIS G Z. Constitutive modeling of dynamic strain aging for HCP metals [J]. European Journal of Mechanics-A: Solids, 2020, 83: 104034. DOI: 10.1016/j.euromechsol.2020.104034.

[12]　ZHANG B, WANG J, WANG Y, et al. Dynamic strain-rate effect on uniaxial tension deformation of Ti5Al2.5Sn α-titanium alloy at various temperatures [J]. Materials at High Temperatures, 2019, 36(6): 479–488. DOI: 10.1080/09603409.2019.1638659.

[13]　RAN J Q, ZHANG G Q, CHEN G P, et al. A multi-strain-rate damage model on fracture prediction in single-point diamond turning process [J]. The International Journal of Advanced Manufacturing Technology, 2020, 110(9): 2753–2765. DOI: 10.1007/s00170-020-06023-0.

[14]　CHEN G, LU L P, REN C Z, et al. Temperature dependent negative to positive strain rate sensitivity and compression behavior for 2024-T351 aluminum alloy [J]. Journal of Alloys and Compounds, 2018, 765: 569–585. DOI: 10.1016/j.jallcom.

2018.06.196.

[15]　JING L, SU X Y, ZHAO L M. The dynamic compressive behavior and constitutive modeling of D1 railway wheel steel over a wide range of strain rates and temperatures [J]. Results in Physics, 2017, 7: 1452–1461. DOI: 10.1016/j.rinp.2017.04.015.

[16]　WEAVER M L, NOEBE R D, KAUFMAN M J. Observations of dynamic strain aging in polycrystalline NiAl [J]. Intermetallics, 1996, 4(8): 593–600. DOI: 10.1016/0966-9795(96)00045-3.

[17]　SAMUEL K G, RAY S K, SASIKALA G. Dynamic strain ageing in prior cold worked 15Cr-15Ni titanium modified stainless steel (Alloy D9) [J]. Journal of Nuclear Materials, 2006, 355(1): 30–37. DOI: 10.1016/j.jnucmat.2006.03.016.

[18]　LI X Y, ROTH C C, MOHR D. Machine-learning based temperature-and rate-dependent plasticity model: application to analysis of fracture experiments on DP steel [J]. International Journal of Plasticity, 2019, 118: 320–344. DOI: 10.1016/j.ijplas.2019.02.012.

[19]　KREYCA J, KOZESCHNIK E. State parameter-based constitutive modelling of stress strain curves in Al-Mg solid solutions [J]. International Journal of Plasticity, 2018, 103: 67–80. DOI: 10.1016/j.ijplas.2018.01.001.

[20]　TSAI C W, LEE C, LIN P T, et al. Portevin-Le Chatelier mechanism in face-centered-cubic metallic alloys from low to high entropy [J]. International Journal of Plasticity, 2019, 122: 212–224. DOI: 10.1016/j.ijplas.2019.07.003.

[21]　WEAVER M L, NOEBE R D, KAUFMAN M J. The influence of C and Si on the flow behavior of NiAl single crystals [J]. Scripta Materialia, 1996, 34(6): 941–948. DOI: 10.1016/1359-6462(95)00590-0.

[22]　CUNIBERTI A. Serrated yielding in long-range ordered 18R Cu-Zn-Al single crystals [J]. Intermetallics, 2006, 14(7): 776–779. DOI: 10.1016/j.intermet.2005.11.011.

[23]　VARADHAN S, BEAUDOIN A J, FRESSENGEAS C. Lattice incompatibility and strain-aging in single crystals [J]. Journal of the Mechanics and Physics of Solids, 2009, 57(10): 1733–1748. DOI: 10.1016/j.jmps.2009.06.007.

[24]　GILAT A, WU X R. Plastic deformation of 1020 steel over a wide range of strain rates and temperatures [J]. International Journal of Plasticity, 1997, 13(6): 611–632. DOI: 10.1016/S0749-6419(97)00028-4.

[25]　ROBINSON J M, SHAW M P. Microstructural and mechanical influences on dynamic strain aging phenomena [J]. International Materials Reviews, 1994, 39(3): 113–122. DOI: 10.1179/imr.1994.39.3.113.

[26]　GIRONÈS A, LLANES L, ANGLADA M, et al. Dynamic strain ageing effects on superduplex stainless steels at intermediate temperatures [J]. Materials Science and Engineering: A, 2004, 367(1): 322–328. DOI: 10.1016/j.msea.2003.10.293.

[27]　孟卫华, 郭伟国, 苏静, 等. DH-36 钢的塑性流动统一本构关系研究 [J]. 力学学报, 2011, 43(5): 958–962. DOI: 10.6052/0459-1879-2011-5-lxxb2010-676.
　　　MENG W H, GUO W G, SU J, et al. Study of plastic flow unified constitutive relation for steel DH-36 [J]. Chinese Journal of Theoretical and Applied Mechanics, 2011, 43(5): 958–962. DOI: 10.6052/0459-1879-2011-5-lxxb2010-676.

[28]　孟卫华, 郭伟国, 王建军, 等. DH36 钢拉伸塑性流动特性及本构关系 [J]. 爆炸与冲击, 2013, 33(4): 438–443. DOI: 10.11883/1001-1455(2013)04-0438-06.
　　　MENG W H, GUO W G, WANG J J, et al. Tensile plasticity flow characteristics of DH36 steel and its constitutive relation [J]. Explosion and Shock Waves, 2013, 33(4): 438–443. DOI: 10.11883/1001-1455(2013)04-0438-06.

[29]　张琼. 低碳钢拉伸形变时影响蓝脆的因素 [J]. 材料科学进展, 1988, 2(6): 87–91.
　　　ZHANG Q. Effect of factor of blue brittle of low-carbon steel for tensile deformation [J]. Materials Science Progress, 1988, 2(6): 87–91.

[30]　LI C C, LESLIE W C. Effects of dynamic strain aging on the subsequent mechanical properties of carbon steels [J]. Metallurgical Transactions A, 1978, 9(12): 1765–1775. DOI: 10.1007/BF02663406.

[31]　HONG S G, Lee S B. The tensile and low-cycle fatigue behavior of cold worked 316L stainless steel: influence of dynamic strain aging [J]. International Journal of Fatigue, 2004, 26(8): 899–910. DOI: 10.1016/j.ijfatigue.2003.12.002.

[32]　RODRIGUEZ P. Serrated plastic flow [J]. Bulletin of Materials Science, 1984, 6(4): 653–663. DOI: 10.1007/BF02743993.

[33]　FU S H, CHENG T, ZHANG Q C, et al. Two mechanisms for the normal and inverse behaviors of the critical strain for the Portevin-Le Chatelier effect [J]. Acta Materialia, 2012, 60(19): 6650–6656. DOI: 10.1016/j.actamat.2012.08.035.

[34]　钱匡武, 彭开萍, 陈文哲. 金属动态应变时效现象中的“锯齿屈服” [J]. 福建工程学院学报, 2003, 1(1): 4–8. DOI: 10.3969/j.issn.1672-4348.2003.01.002.
　　　QIAN K W, PENG K P, CHEN W Z. Features of serrated yielding of dynamic strain aging phenomenon in metals and alloys [J]. Journal of Fujian University of Technology, 2003, 1(1): 4–8. DOI: 10.3969/j.issn.1672-4348.2003.01.002.

[35] YILMAZ A. The Portevin–Le Chatelier effect: a review of experimental findings [J]. Science and Technology of Advanced Materials, 2011, 12(6): 063001. DOI: 10.1088/1468-6996/12/6/063001.

[36] SAKTHIVEL T, LAHA K, NANDAGOPAL M, et al. Effect of temperature and strain rate on serrated flow behaviour of Hastelloy X [J]. Materials Science and Engineering: A, 2012, 534: 580–587. DOI: 10.1016/j.msea.2011.12.011.

[37] ROY A K, PAL J, MUKHOPADHYAY C. Dynamic strain ageing of an austenitic superalloy—Temperature and strain rate effects [J]. Materials Science and Engineering: A, 2008, 474(1): 363–370. DOI: 10.1016/j.msea.2007.05.056.

[38] KARABULUT H, GÜNDÜZ S. Effect of vanadium content on dynamic strain ageing in microalloyed medium carbon steel [J]. Materials & Design, 2004, 25(6): 521–527. DOI: 10.1016/j.matdes.2004.01.005.

[39] GÜNDÜZ S, ACARER M. The effect of heat treatment on high temperature mechanical properties of microalloyed medium carbon steel [J]. Materials & Design, 2006, 27(10): 1076–1085. DOI: 10.1016/j.matdes.2005.01.020..

[40] XIAO J Y, WANG J J, GUO W G, et al. The influence of heat treatment and strain rate on the third type strain ageing phenomenon [J]. Materials at High Temperatures, 2019, 36(2): 104–110. DOI: 10.1080/09603409.2018.1467108.

[41] YUAN K B, GUO W G, LI D W, et al. Influence of heat treatments on plastic flow of laser deposited Inconel 718: testing and microstructural based constitutive modeling [J]. International Journal of Plasticity, 2021, 136: 102865. DOI: 10.1016/j.ijplas.2020.102865.

[42] YUAN K B, GUO W G, LI P H, et al. Thermomechanical behavior of laser metal deposited inconel 718 superalloy over a wide range of temperature and strain rate: testing and constitutive modeling [J]. Mechanics of Materials, 2019, 135: 13–25. DOI: 10.1016/j.mechmat.2019.04.024.

[43] MCCORMIGK P G. A model for the Portevin-Le Chatelier effect in substitutional alloys [J]. Acta Metallurgica, 1972, 20(3): 351–354. DOI: 10.1016/0001-6160(72)90028-4.

[44] VAN DEN BEUKEL A, KOCKS U F. The strain dependence of static and dynamic strain-aging [J]. Acta Metallurgica, 1982, 30(5): 1027–1034. DOI: 10.1016/0001-6160(82)90211-5.

[45] COTTRELL A H. LXXXVI. A note on the Portevin-Le Chatelier effect [J]. The London, Edinburgh, and Dublin Philosophical Magazine and Journal of Science, 1953, 44(355): 829–832. DOI: 10.1080/14786440808520347.

[46] CUDDY L J, LESLIE W C. Some aspects of serrated yielding in substitutional solid solutions of iron [J]. Acta Metallurgica, 1972, 20(10): 1157–1167. DOI: 10.1016/0001-6160(72)90164-2.

[47] SCHWARZ R B, FUNK L L. Kinetics of the Portevin-Le Chatelier effect in Al 6061 alloy [J]. Acta Metallurgica, 1985, 33(2): 295–307. DOI: 10.1016/0001-6160(85)90148-8.

[48] PICU R C, ZHANG D. Atomistic study of pipe diffusion in Al-Mg alloys [J]. Acta Materialia, 2004, 52(1): 161–171. DOI: 10.1016/j.actamat.2003.09.002.

[49] PENG K P, QIAN K W, CHEN W Z. Effect of dynamic strain aging on high temperature properties of austenitic stainless steel [J]. Materials Science and Engineering: A, 2004, 379(1): 372–377. DOI: 10.1016/j.msea.2004.03.004.

[50] CORBY C, CÁCERES C H, LUKÁČ P. Serrated flow in magnesium alloy AZ91 [J]. Materials Science and Engineering: A, 2004, 387: 22–24. DOI: 10.1016/j.msea.2004.01.077.

[51] FRIEDEL J. Dislocations: international series of monographs on solid state physics [M]. Oxford: Pergamon Press, 1964: 491.

[52] LEE M H, KIM J H, CHOI B K, et al. Mechanical properties and dynamic strain aging behavior of Zr-1.5Nb-0.4Sn-0.2Fe alloy [J]. Journal of Alloys and Compounds, 2007, 428(1/2): 99–105. DOI: 10.1016/j.jallcom.2006.03.076.

[53] 钱匡武, 李效琦, 萧林钢, 等. 金属和合金中的动态应变时效现象 [J]. 福州大学学报 (自然科学版), 2001, 29(6): 8–23. DOI: 10.3969/j.issn.1000-2243.2001.06.003.
QIAN K W, LI X Q, XIAO L G, et al. Dynamic strain aging phenomenon in metals and alloys [J]. Journal of Fuzhou University (Natural Science), 2001, 29(6): 8–23. DOI: 10.3969/j.issn.1000-2243.2001.06.003.

[54] 张质良, 余大伟, 阮雪榆. "蓝脆" 温度挤压特性的研究 [J]. 模具技术, 1983(2): 1–13.

[55] 王敏杰, 胡荣生, 刘培德. 金属切削中的蓝脆效应与热塑剪切失稳 [J]. 科学通报, 1990, 35(8): 634–636. DOI: 10.1360/csb1990-35-8-634.

[56] KIM I S, KANG S S. Dynamic strain aging in SA508-class 3 pressure vessel steel [J]. International Journal of Pressure Vessels and Piping, 1995, 62(2): 123–129. DOI: 10.1016/0308-0161(95)93969-C.

[57] CAILLARD D. Dynamic strain ageing in iron alloys: the shielding effect of carbon [J]. Acta Materialia, 2016, 112: 273–284. DOI: 10.1016/j.actamat.2016.04.018.

[58]　KOYAMA M, SHIMOMURA Y, CHIBA A, et al. Room-temperature blue brittleness of Fe-Mn-C austenitic steels [J]. Scripta Materialia, 2017, 141: 20–23. DOI: 10.1016/j.scriptamat.2017.07.017.

[59]　VERMA P, RAO G S, CHELLAPANDI P, et al. Dynamic strain ageing, deformation, and fracture behavior of modified 9Cr-1Mo steel [J]. Materials Science and Engineering: A, 2015, 621: 39–51. DOI: 10.1016/j.msea.2014.10.011.

[60]　SCHWINK C, NORTMANN A. The present experimental knowledge of dynamic strain ageing in binary f.c.c. solid solutions [J]. Materials Science and Engineering: A, 1997, 234(97): 1–7. DOI: 10.1016/S0921-5093(97)00139-1.

[61]　WOLFENDEN A, KINRA V K. M3D III: mechanics and mechanisms of materials damping [M]. West Conshohocken, PA: ASTM International, 1997.

[62]　MARTIN R, TKALCEC I, MARI D, et al. Tempering effects on three martensitic carbon steels studied by mechanical spectroscopy [J]. Philosophical Magazine, 2008, 88(22): 2907–2920. DOI: 10.1080/14786430802406249.

[63]　TKALCEC I, MARI D. Internal friction in martensitic, ferritic and bainitic carbon steel; cold work effects [J]. Materials Science and Engineering: A, 2004, 370(1): 213–217. DOI: 10.1016/j.msea.2003.04.004.

[64]　TKALCEC I, MARI D, BENOIT W. Correlation between internal friction background and the concentration of carbon in solid solution in a martensitic steel [J]. Materials Science and Engineering: A, 2006, 442(1): 471–475. DOI: 10.1016/j.msea.2006.03.115.

[65]　NIEMEYER T C, GRANDINI C R, FLORÊNCIO O. Stress-induced ordering due heavy interstitial atoms in Nb–0.3 wt.% Ti alloys [J]. Materials Science and Engineering: A, 2005, 396(1): 285–289. DOI: 10.1016/j.msea.2005.01.045.

[66]　STRAHL A, GOLOVINA S B, GOLOVIN I S, et al. On dislocation-related internal friction in Fe-22-31 at.% Al [J]. Journal of Alloys and Compounds, 2004, 378(1): 268–273. DOI: 10.1016/j.jallcom.2003.10.066.

[67]　郭伟国, 左红星, 孟卫华, 等. 第三种应变时效与机械波谱关联性探讨 [J]. 材料科学与工艺, 2012, 20(1): 128–134, 127. DOI: 10.11951/j.issn.1005-0299.20120126.
GUO W G, ZUO H X, MENG W H, et al. Discussion of the relevancy of the third-type strain aging and mechanical spectroscopy [J]. Materials Science and Technology, 2012, 20(1): 128–134, 127. DOI: 10.11951/j.issn.1005-0299.20120126.

[68]　彭开萍, 陈文哲, 钱匡武. 3004 铝合金"反常"锯齿屈服现象的研究 [J]. 物理学报, 2006, 55(7): 3569–3575. DOI: 10.3321/j.issn:1000-3290.2006.07.061.
PENG K P, CHEN W Z, QIAN K W. Study of an anomalous serrated yielding phenomenon in 3004 aluminum alloy [J]. Acta Physica Sinica, 2006, 55(7): 3569–3575. DOI: 10.3321/j.issn:1000-3290.2006.07.061.

[69]　LEE S J, KIM J, KANE S N, et al. On the origin of dynamic strain aging in twinning-induced plasticity steels [J]. Acta Materialia, 2011, 59(17): 6809–6819. DOI: 10.1016/j.actamat.2011.07.040.

[70]　KARLSEN W, IVANCHENKO M, EHRNSTÉN U, et al. Microstructural manifestation of dynamic strain aging in AISI 316 stainless steel [J]. Journal of Nuclear Materials, 2009, 395(1): 156–161. DOI: 10.1016/j.jnucmat.2009.10.047.

[71]　IVANCHENKO M, NEVDACHA V, YAGODZINSKYY Y, et al. Internal friction studies of carbon and its redistribution kinetics in Inconel 600 and 690 alloys under dynamic strain aging conditions [J]. Materials Science and Engineering: A, 2006, 442(1): 458–461. DOI: 10.1016/j.msea.2006.02.207.

[72]　JOHNSON G R, COOK W H. A constitutive model and date for metals subjected to large strains, high strain rates, and high temperatures [C] // Proceedings of the 7th International Symposium on Ballistics. The Hague, Netherlands, 1983: 541−547.

[73]　LIANG R Q, KHAN A S. A critical review of experimental results and constitutive models for BCC and FCC metals over a wide range of strain rates and temperatures [J]. International Journal of Plasticity, 1999, 15(9): 963–980. DOI: 10.1016/S0749-6419(99)00021-2.

[74]　RULE W K, JONES S E. A revised form for the Johnson-Cook strength model [J]. International Journal of Impact Engineering, 1998, 21(8): 609–624. DOI: 10.1016/S0734-743X(97)00081-X.

[75]　ZERILLI F J, ARMSTRONG R W. Dislocation-mechanics-based constitutive relations for material dynamics calculations [J]. Journal of Applied Physics, 1987, 61(5): 1816–1825. DOI: 10.1063/1.338024.

[76]　FOLLANSBEE P S, KOCKS U F. A constitutive description of the deformation of copper based on the use of the mechanical threshold stress as an internal state variable [J]. Acta Metallurgica, 1988, 36(1): 81–93. DOI: 10.1016/0001-6160(88)90030-2.

[77]　BODNER S R, PARTOM Y. Constitutive equations for elastic-viscoplastic strain-hardening materials [J]. Journal of Applied Mechanics, 1975, 42(2): 385–389. DOI: 10.1115/1.3423586.

[78]　NEMAT-NASSER S, GUO W G, CHENG J Y. Mechanical properties and deformation mechanisms of a commercially pure

titanium [J]. Acta Materialia, 1999, 47(13): 3705–3720. DOI: 10.1016/S1359-6454(99)00203-7.

[79] NEMAT-NASSER S, GUO W G. High strain-rate response of commercially pure vanadium [J]. Mechanics of Materials, 2000, 32(4): 243–260. DOI: 10.1016/S0167-6636(99)00056-3.

[80] RUSINEK A, KLEPACZKO J R. Shear testing of a sheet steel at wide range of strain rates and a constitutive relation with strain-rate and temperature dependence of the flow stress [J]. International Journal of Plasticity, 2001, 17(1): 87–115. DOI: 10.1016/S0749-6419(00)00020-6.

[81] GAO C Y, ZHANG L C. Constitutive modelling of plasticity of fcc metals under extremely high strain rates [J]. International Journal of Plasticity, 2012, 32: 121–133. DOI: 10.1016/j.ijplas.2011.12.001.

[82] KHAN A S, LIU H W. Variable strain rate sensitivity in an aluminum alloy: response and constitutive modeling [J]. International Journal of Plasticity, 2012, 35: 1–14. DOI: 10.1016/j.ijplas.2012.02.001.

[83] CHENG J Y, NEMAT-NASSER S. A model for experimentally-observed high-strain-rate dynamic strain aging in titanium [J]. Acta Materialia, 2000, 48(12): 3131–3144. DOI: 10.1016/S1359-6454(00)00124-5.

[84] HONG S I. Influence of dynamic strain aging on the apparent activation volume for deformation [J]. Materials Science and Engineering, 1985, 76: 77–81. DOI: 10.1016/0025-5416(85)90082-5.

[85] LEE K W, KIM S K, KIM K T, et al. Ductility and strain rate sensitivity of Zircaloy-4 nuclear fuel claddings [J]. Journal of Nuclear Materials, 2001, 295(1): 21–26. DOI: 10.1016/S0022-3115(01)00509-8.

[86] LEE K O, LEE S B. Modeling of materials behavior at various temperatures of hot isostatically pressed superalloys [J]. Materials Science and Engineering: A, 2012, 541: 81–87. DOI: 10.1016/j.msea.2012.02.005.

[87] SU J, GUO W, MENG W, et al. Plastic behavior and constitutive relations of DH-36 steel over a wide spectrum of strain rates and temperatures under tension [J]. Mechanics of Materials, 2013, 65: 76–87. DOI: 10.1016/j.mechmat.2013.06.002.

[88] SHEN F H, MÜNSTERMANN S, LIAN J H. An evolving plasticity model considering anisotropy, thermal softening and dynamic strain aging [J]. International Journal of Plasticity, 2020, 132: 102747. DOI: 10.1016/j.ijplas.2020.102747.

[89] 郭扬波, 唐志平, 程经毅. 一种基于位错机制的动态应变时效模型 [J]. 固体力学学报, 2002, 23(3): 249–256. DOI: 10.3969/j.issn.0254-7805.2002.03.001.
GUO Y B, TANG Z P, CHENG J Y. A dislocation-mechanics-based constitutive model for dynamic strain aging [J]. Acta Mechanica Solida Sinica, 2002, 23(3): 249–256. DOI: 10.3969/j.issn.0254-7805.2002.03.001.

[90] VOYIADJIS G Z, SONG Y, RUSINEK A. Constitutive model for metals with dynamic strain aging [J]. Mechanics of Materials, 2019, 129: 352–360. DOI: 10.1016/j.mechmat.2018.12.012.

[91] VOYIADJIS G Z, SONG Y. A physically based constitutive model for dynamic strain aging in inconel 718 alloy at a wide range of temperatures and strain rates [J]. Acta Mechanica, 2020, 231(1): 19–34. DOI: 10.1007/s00707-019-02508-6.

(责任编辑　曾月蓉)